Methane Activation

DOI: 10.1002/anie.201201698

Thermal Reactions of $YAlO_3^{+\bullet}$ with Methane: Increasing the Reactivity of $Y_2O_3^{+\bullet}$ and the Selectivity of $Al_2O_3^{+\bullet}$ by Doping**

Jia-Bi Ma, Zhe-Chen Wang, Maria Schlangen, Sheng-Gui He,* and Helmut Schwarz**

Dedicated to Professor Bernhard Kräutler on the occasion of his 65th birthday

Methane, the major component of natural gas, constitutes one of the major energy sources and an important feedstock for the synthesis of value-added products.[1] Owing to the substantial economic benefits and scientific challenge, the functionalization of methane at ambient conditions has formed a subject of intense research in contemporary chemistry. Heterogeneous catalysis mediated by metal oxides is one of the most efficient ways to activate the inert C–H bond of methane.[2] In addition, γ-Al_2O_3 catalyzes H/D exchange reactions of D_2/CH_4 and CH_4/CD_4 mixtures,[3] and with the assistance of H_2O, the reactivity of γ-Al_2O_3 in terms of the C–H bond activation of methane can be increased.[4] Yttrium and yttria are also used as catalytic promoters or supports in methane oxidation.[2a,5]

Studies on the gas-phase reactions of metal-oxide clusters with methane can provide meaningful insight concerning the elementary steps of catalytic processes, and may help to design new efficient catalysts.[6] Hydrogen-atom transfer (HAT) from CH_4 is viewed as the decisive step in the oxidative dimerization of methane.[7] Numerous oxide-cluster cations which contain terminal oxygen-centered radicals ($O_t^{\bullet}$, with spin density close to 1 μ_B) act as active sites to generate $CH_3^{\bullet}$; these include not only homonuclear metal-oxide clusters such as $MgO^{+\bullet}$,[8] $FeO^{+\bullet}$,[9] $MoO^{+\bullet}$,[10] $ReO_3(OH)^{+\bullet}$,[11] $OsO^{+\bullet}$,[12] $V_4O_{10}^{+\bullet}$,[13] $(Al_2O_3)_x^{+\bullet}$ $(x=3–5)$,[14] $Al_2O_7^{+\bullet}$,[15] and others,[16] but also the metal-free oxides $SO_2^{+\bullet}$[17] and $P_4O_{10}^{+\bullet}$,[18] as well as heteronuclear oxide clusters such as $AlVO_4^{+\bullet}$,[19] $V_xP_{4-x}O_{10}^{+\bullet}$ $(x=2,3)$,[20] $V_2O_5(SiO_2)_x^{+\bullet}$ $(x=1–4)$,[21] and $V_{4-x}Y_xO_{10-x}^{+\bullet}$ $(x=1,2)$.[22,23]

Recently, detailed theoretical and experimental studies demonstrated that $Y_2O_3^{+\bullet}$ is not capable of bond activation of methane at low temperature because it lacks an $O_t^{\bullet}$ site.[16,24] According to density functional theory (DFT) calculations, the unpaired spin density in $Y_2O_3^{+\bullet}$ is delocalized over two bridging oxygen atoms (0.57 μ_B on each O_b atom).[24] Aluminum and yttrium are both typical trivalent metal elements in the periodic table. However, $Al_2O_3^{+\bullet}$, possessing exactly the same stoichiometry as $Y_2O_3^{+\bullet}$, does react at room temperature with methane to produce a methyl radical (HAT) and formaldehyde with a branching ratio of 35:65 [Reactions (1) and (2)] and an overall reaction efficiency of roughly 7 %.[25] In contrast to $Y_2O_3^{+\bullet}$, $Al_2O_3^{+\bullet}$ possesses an $O_t^{\bullet}$ unit according to DFT calculations.[15]

$$Al_2O_3^{+\bullet} + CH_4 \rightarrow Al_2O_3H^+ + CH_3^{\bullet} \quad (1)$$

$$Al_2O_3^{+\bullet} + CH_4 \rightarrow Al_2O_2H_2^+ + CH_2O \quad (2)$$

$$Y_2O_3^{+\bullet} + CH_4 \not\rightarrow \quad (3)$$

Thus, it may be of interest and instructive to address the reactivity of aluminum-doped yttrium oxide clusters possessing the stoichiometry of the reactive aluminum and the inert yttrium oxide, that is, $YAlO_3^{+\bullet}$, toward methane to elucidate the doping effect on the bond activation of methane.[6b]

To this end, the heteronuclear oxide cluster $YAlO_3^{+\bullet}$ was generated and its reaction with CH_4 was studied experimentally and theoretically. Figure 1 plots the Fourier-transform ion-cyclotron resonance (FT-ICR) mass spectra, showing the

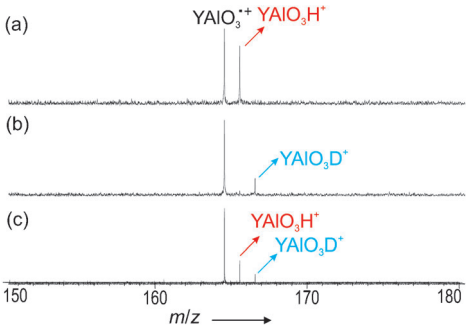

Figure 1. Mass spectra showing the reactions of $YAlO_3^{+\bullet}$ with a) CH_4 at a pressure of 4×10^{-8} mbar after a reaction time of 4 s, b) CD_4 at a pressure of 4×10^{-8} mbar after a reaction time of 4 s, c) CH_2D_2 at a pressure of 7×10^{-8} mbar after a reaction time of 2 s.

[*] J.-B. Ma, Dr. Z.-C. Wang, Dr. M. Schlangen, Prof. Dr. H. Schwarz
Institut für Chemie, Technische Universität Berlin
Strasse des 17. Juni 135, 10623 Berlin (Germany)
E-mail: maria.schlangen@mail.chem.tu-berlin.de
helmut.schwarz@mail.chem.tu-berlin.de
Prof. Dr. H. Schwarz
Chemistry Department, Faculty of Science
King Abdulaziz University, Jeddah 21589 (Saudi Arabia)
E-mail: hschwarz@kau.edu.sa
J.-B. Ma, Prof. Dr. S.-G. He
State Key Laboratory for Structural Chemistry of Unstable and Stable Species, Institute of Chemistry, Chinese Academy of Sciences
100190, Beijing (P.R. China)
E-mail: shengguihe@iccas.ac.cn

[**] This work was supported by the Fonds der Chemischen Industrie, the Deutsche Forschungsgemeinschaft (DFG), and the Cluster of Excellence "Unifying Concepts in Catalysis" (coordinated by the Technische Universität Berlin and funded by the DFG). For computational resources, the Institut für Mathematik at the Technische Universität Berlin is acknowledged. We thank Dr. Xunlei Ding and Nicolas Dietl for helpful suggestions and discussions.

reaction of thermalized, mass-selected $YAlO_3^{+\bullet}$ with methane. As apparent from the figure, $YAlO_3^{+\bullet}$ brings about efficient HAT at room temperature [Reaction (4)].

$$YAlO_3^{+\bullet} + CH_4 \rightarrow YAlO_3H^+ + CH_3^{\bullet} \quad (4)$$

The rate constant of $k(YAlO_3^{+\bullet}+CH_4)$ has been determined to be 1.05×10^{-10} $cm^3 s^{-1}$ $molecule^{-1}$, corresponding to an efficiency of 11 %.[26] The intramolecular kinetic isotope effect (KIE) derived from the $YAlO_3^{+\bullet}/CH_2D_2$ system amounts to 2.3 ± 0.2. Thus, HAT reactivity is observed for $YAlO_3^{+\bullet}$ in contrast to $Y_2O_3^{+\bullet}$. Further, the heteronuclear system is at least as reactive as $Al_2O_3^{+\bullet}$ with respect to this reaction channel. However, the second reaction channel observed for the $Al_2O_3^{+\bullet}/CH_4$ system, that is, formation of formaldehyde, is suppressed in the $YAlO_3^{+\bullet}/CH_4$ couple.

DFT calculations have been carried out to explain the different reactivities of $YAlO_3^{+\bullet}$ and its homonuclear analogues; to this end, the mechanisms of HAT from methane as well as of the formaldehyde formation have been investigated computationally. Similar to $Al_2O_3^{+\bullet}$, the lowest-energy structure of $YAlO_3^{+\bullet}$ has an Y-O-Al-O four-membered-ring with an $O_t^{\bullet}$ unit bound to the Al atom (with the spin density indicated by the blue isosurface in **1**, Figure 2). The corresponding isomer with an $O_t^{\bullet}$ unit bound to the Y atom is

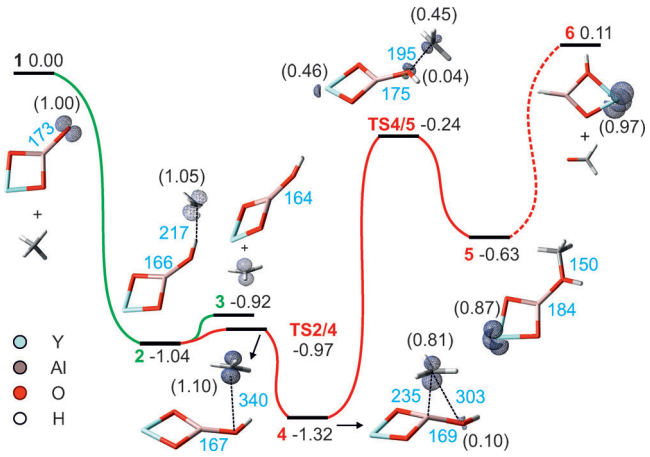

Figure 2. The potential energy profiles for the reaction of $YAlO_3^{+\bullet}$ with methane. The energies (given in eV) are relative to the entrance channel and corrected for zero-point vibrational energy contributions. Some key bond lengths are given in pm (in blue). The unpaired spin-density distributions are shown in the blue isosurface, and the values in μ_B are given in parentheses. The details of the reaction steps connecting **5** and **6** are not calculated.

1.99 eV higher in energy and therefore not included in the following discussion.

HAT from methane to $O_t^{\bullet}$ of the $YAlO_3^{+\bullet}$ cluster (**1**→**2**→**3**) is thermodynamically favorable and overall barrierless. No encounter complex $YAlO_3^{+\bullet}\cdot CH_4$ can be located on the potential energy surface (PES); HAT from CH_4 to $YAlO_3^{+\bullet}$ results directly in the formation of intermediate **2**, in which $CH_3^{\bullet}$ is loosely coordinated to the newly formed hydroxy group. This complex can dissociate into $YAlO_3H^+$ and $CH_3^{\bullet}$ (product **3**, Figure 2).

An interesting question is raised by these results: why does the presence of yttrium increase the selectivity of $YAlO_3^{+\bullet}$ over that of $Al_2O_3^{+\bullet}$, though $YAlO_3^{+\bullet}$ and $Al_2O_3^{+\bullet}$ possess similar aluminum-bound $O_t^{\bullet}$ units serving as the reactive site? In the $Al_2O_3^{+\bullet}/CH_4$ system, the methanol complex $[Al_2O_2(HOCH_3)]^+$ (intermediate **7**, Figure 3) is

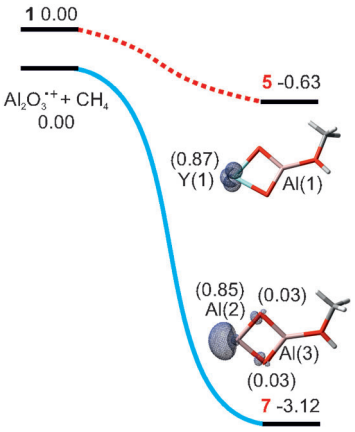

Figure 3. The potential energy profiles for Reaction (5). The energies (given in eV) are relative to the entrance channel and corrected by zero-point vibrational energies. The unpaired spin-density distributions of $[XAlO_2(HOCH_3)]^+$ (X = Y or Al) are shown in the blue isosurface, and the values (in the parentheses) in μ_B are given. The formation of **5** from **1** is indicated by a dotted red line and involves the HAT from methane to the cluster (**1**→**2**), the transfer of the $CH_3^{\bullet}$ moiety (**2**→**TS2/4**→**4**) and the formation of the C–O bond (**4**→**TS4/5**→**5**); see Figure 2 for details.

formed directly by insertion of the terminal oxygen atom of $Al_2O_3^{+\bullet}$ into the C–H bond of methane according to Reaction (5) (X = Al), and there is sufficient energy (−3.12 eV with respect to the reactants) gained in this step to surmount the following reaction barriers to generate formaldehyde.[25] In sharp contrast, the analogous intermediate **5** of the mixed system is only 0.63 eV lower in energy than the reactants (Figure 3); moreover, it is accessible only via the energetically high-lying transition state **TS4/5** (−0.24 eV) which is located well above the exit channel to produce in an entropy-favored reaction the HAT products **3**/$CH_3^{\bullet}$. Further, the loss of methanol from intermediates **5** and **7** yielding $Y(\mu\text{-}O)_2Al^+$ and $Al(\mu\text{-}O)_2Al^+$, respectively, is much more energy demanding for the former, that is, 2.83 eV compared to 1.02 eV for the latter, thus reflecting the relative low stability of **7** compared to **5**.

$$X^{III}Al^{III}O_3^{+\bullet} + CH_4 \rightarrow [X^{II}Al^{III}O_2(HOCH_3)]^+ \ (X = Y \text{ or } Al) \quad (5)$$

This drastic distinction is caused by the different intrinsic properties of yttrium and aluminum. As shown in Figure 3, the unpaired electron in $[Al_2O_2(HOCH_3)]^+$ and $[YAlO_2(HOCH_3)]^+$ is located on Al(2) and Y(1), respectively; thus, these atoms are reduced in the reaction step $[XAlO_3]^{+\bullet} + CH_4 \rightarrow [XAlO_2(HOCH_3)]^+$, as indicated in Reaction (5). The second/third ionization energies (IE) of Y and Al amount to 12.23/20.52 eV and 18.83/28.45 eV, respectively.[27] Therefore,

more energy is released in the reduction of $Al_2O_3^{+\bullet}$ in Reaction (5) than in the reduction of $YAlO_3^{+\bullet}$ forming $[YAlO_2(HOCH_3)]^+$ (**5**); thus, $[YAlO_2(HOCH_3)]^+$ is much less stable than $[Al_2O_2(HOCH_3)]^+$ (**7**). Furthermore, the energy gain in the formation of **5** is not high enough to overcome the subsequent barriers to generate formaldehyde as shown in Figure 2.[28]

To the best of our knowledge, $YAlO_3^{+\bullet}$ is the smallest transition-metal heteronuclear oxide cluster that is reactive toward methane at room temperature. Our experimental and theoretical studies demonstrate that the inert yttrium oxide cluster doped with aluminum brings about efficient methane activation at room temperature. At the same time, the reaction pattern of $YAlO_3^{+\bullet}$ is quite different from that of $Al_2O_3^{+\bullet}$ as a result of the doping effect. In summary, the heteronuclear oxide cluster $YAlO_3^{+\bullet}$ exhibits an increased reactivity and selectivity compared with the homonuclear analogues $Y_2O_3^{+\bullet}$ and $Al_2O_3^{+\bullet}$, respectively, in the reaction with methane.

Experimental Section

All experiments were performed with a Spectrospin CMS 47X FTICR mass spectrometer equipped with an external ion source as described elsewhere.[29] In brief, cluster cations $YAlO_2^{+\bullet}$ were generated by laser ablation of an yttrium/aluminium target (with the molar ratio of 1:1) using a Nd:YAG laser operating at 1064 nm in the presence of 0.5 % O_2 seeded in helium carrier gas. Using a series of potentials and ion lenses, the ions were transferred into the ICR cell which was positioned in the bore of a 7.05 T superconducting magnet. Next the mass-selected cluster $YAlO_2^{+\bullet}$ was reacted with pulsing N_2O (ca. 2×10^{-6} mbar) in the ICR cell to generate $YAlO_3^{+\bullet}$. After collisional thermalization by pulses of argon (ca. 2×10^{-6} mbar), the $YAlO_3^{+\bullet}$ cluster was mass-selected and studied with respect to the reactivity toward methane by introducing the substrate through a leak-valve. The experimental second-order rate constants were evaluated assuming a pseudo-first-order kinetic approximation after calibration of the measured pressure and acknowledgment of the ion-gauge sensitivities. The rate constants have an uncertainty of ±30 %.[30] For the thermalized cluster ions a temperature of 298 K was assumed.[30]

The DFT calculations were carried out using the Gaussian 09 program[31] employing the hybrid B3LYP exchange-correlation functional.[32] TZVP basis sets[33] were selected for Al, C, H, O atoms, and polarized triple-ζ valence basis sets (Def2-TZVP)[34] were selected for Y. Geometry optimizations with full relaxation of all atoms were performed. Vibrational frequency calculations were performed to check that the reaction intermediates have zero imaginary frequency. The energies (given in eV) were corrected by zero-point vibrational energy. Intrinsic reaction-coordinate (IRC) calculations[35] were also performed to connect the transition state with local minima.

Received: March 2, 2012
Published online: May 4, 2012

Keywords: C–H activation · gas-phase reactions · mass spectrometry · radicals

[1] G. A. Olah, *Angew. Chem.* **2005**, *117*, 2692; *Angew. Chem. Int. Ed.* **2005**, *44*, 2636.
[2] a) R. Q. Long, H. L. Wan, *Appl. Catal. A* **1997**, *159*, 45; b) H. Launay, S. Loridant, D. L. Nguyen, A. M. Volodin, J. L. Dubois, J. M. M. Millet, *Catal. Today* **2007**, *128*, 176.
[3] J. G. Larson, W. K. Hall, *J. Phys. Chem.* **1965**, *69*, 3080.
[4] R. Wischert, C. Copéret, F. Delbecq, P. Sautet, *Angew. Chem.* **2011**, *123*, 3260; *Angew. Chem. Int. Ed.* **2011**, *50*, 3202.
[5] J. J. Zhu, J. G. van Ommen, H. J. M. Bouwmeester, L. Lefferts, *J. Catal.* **2005**, *233*, 434.
[6] a) X.-L. Ding, X.-N. Wu, Y.-X. Zhao, S.-G. He, *Acc. Chem. Res.* **2012**, *45*, 382; b) H. Schwarz, *Angew. Chem.* **2011**, *123*, 10276; *Angew. Chem. Int. Ed.* **2011**, *50*, 10096; c) J. Roithová, D. Schröder, *Chem. Rev.* **2010**, *110*, 1170; d) G. E. Johnson, R. Mitrić, V. Bonačić-Koutecký, A. W. Castleman, Jr., *Chem. Phys. Lett.* **2009**, *475*, 1; e) D. Schröder, H. Schwarz, *Proc. Natl. Acad. Sci. USA* **2008**, *105*, 18114; f) D. K. Böhme, H. Schwarz, *Angew. Chem.* **2005**, *117*, 2388; *Angew. Chem. Int. Ed.* **2005**, *44*, 2336.
[7] a) A. A. Fokin, P. R. Schreiner, *Adv. Synth. Catal.* **2003**, *345*, 1035; b) J. H. Lunsford, *Catal. Today* **2000**, *63*, 165; c) M. Lersch, M. Tilset, *Chem. Rev.* **2005**, *105*, 2471.
[8] D. Schröder, J. Roithová, *Angew. Chem.* **2006**, *118*, 5835; *Angew. Chem. Int. Ed.* **2006**, *45*, 5705.
[9] D. Schröder, A. Fiedler, J. Hrušák, H. Schwarz, *J. Am. Chem. Soc.* **1992**, *114*, 1215.
[10] I. Kretzschmar, A. Fiedler, J. N. Harvey, D. Schröder, H. Schwarz, *J. Phys. Chem. A* **1997**, *101*, 6252.
[11] M. K. Beyer, C. B. Berg, V. E. Bondybey, *Phys. Chem. Chem. Phys.* **2001**, *3*, 1840.
[12] K. K. Irikura, J. L. Beauchamp, *J. Am. Chem. Soc.* **1989**, *111*, 75.
[13] S. Feyel, J. Döbler, D. Schröder, J. Sauer, H. Schwarz, *Angew. Chem.* **2006**, *118*, 4797; *Angew. Chem. Int. Ed.* **2006**, *45*, 4681.
[14] S. Feyel, J. Döbler, R. Höckendorf, M. K. Beyer, J. Sauer, H. Schwarz, *Angew. Chem.* **2008**, *120*, 1972; *Angew. Chem. Int. Ed.* **2008**, *47*, 1946.
[15] Z.-C. Wang, T. Weiske, R. Kretschmer, M. Schlangen, M. Kaupp, H. Schwarz, *J. Am. Chem. Soc.* **2011**, *133*, 16930.
[16] Y. X. Zhao, X. N. Wu, Z. C. Wang, S. G. He, X. L. Ding, *Chem. Commun.* **2010**, *46*, 1736.
[17] G. de Petris, A. Troiani, M. Rosi, G. Angelini, O. Ursini, *Chem. Eur. J.* **2009**, *15*, 4248.
[18] N. Dietl, M. Engeser, H. Schwarz, *Angew. Chem.* **2009**, *121*, 4955; *Angew. Chem. Int. Ed.* **2009**, *48*, 4861.
[19] Z.-C. Wang, X.-N. Wu, Y.-X. Zhao, J.-B. Ma, X.-L. Ding, S.-G. He, *Chem. Phys. Lett.* **2010**, *489*, 25.
[20] a) J.-B. Ma, X.-N. Wu, Y.-X. Zhao, X.-L. Ding, S.-G. He, *Phys. Chem. Chem. Phys.* **2010**, *12*, 12223; b) N. Dietl, R. F. Höckendorf, M. Schlangen, M. Lerch, M. K. Beyer, H. Schwarz, *Angew. Chem.* **2011**, *123*, 1466; *Angew. Chem. Int. Ed.* **2011**, *50*, 1430.
[21] X.-L. Ding, Y.-X. Zhao, X.-N. Wu, Z.-C. Wang, J.-B. Ma, S.-G. He, *Chem. Eur. J.* **2010**, *16*, 11463.
[22] Z.-Y. Li, Y.-X. Zhao, X.-N. Wu, X.-L. Ding, S.-G. He, *Chem. Eur. J.* **2011**, *17*, 11728.
[23] For recent reviews on HAT, see: a) Ref. [6a]; b) N. Dietl, M. Schlangen, H. Schwarz, *Angew. Chem.* **2012**, DOI: 10.1002/ange.201108363; *Angew. Chem. Int. Ed.* **2012**, DOI: 10.1002/anie.201108363.
[24] Y. X. Zhao, X. L. Ding, Y. P. Ma, Z. C. Wang, S. G. He, *Theor. Chem. Acc.* **2010**, *127*, 449.
[25] Z.-C. Wang, R. Kretschmer, N. Dietl, J.-B. Ma, T. Weiske, M. Schlangen, H. Schwarz, *Angew. Chem.* **2012**, *124*, 3763 – 3767; *Angew. Chem. Int. Ed.* **2012**, *51*, 3703 – 3707.
[26] T. Su, M. T. Bowers, *J. Chem. Phys.* **1973**, *58*, 3027.
[27] http://www.webelements.com/aluminium/atoms.html, and http://www.webelements.com/yttrium/atoms.html.
[28] The structure of the $YAlO_2H_2^{+\bullet}$ cluster shown in Figure 2 is the lowest-energy structure according to the DFT calculations; the

isomers $[HY(\mu\text{-}OH)(\mu\text{-}O)Al]^+$ and $[Y(\mu\text{-}OH)_2Al]^+$ are higher in energy by 0.73 eV and 0.68 eV, respectively.

[29] a) K. Eller, H. Schwarz, *Int. J. Mass Spectrom. Ion Processes* **1989**, *93*, 243; b) K. Eller, W. Zummack, H. Schwarz, *J. Am. Chem. Soc.* **1990**, *112*, 621; c) M. Engeser, D. Schröder, T. Weiske, H. Schwarz, *J. Phys. Chem. A* **2003**, *107*, 2855.

[30] D. Schröder, H. Schwarz, D. E. Clemmer, Y. M. Chen, P. B. Armentrout, V. I. Baranov, D. K. Bohme, *Int. J. Mass Spectrom. Ion Processes* **1997**, *161*, 175.

[31] Gaussian 09 (Revision A.02), M. J. Frisch, et al., Gaussian, Inc., Wallingford CT, **2009**.

[32] a) A. D. Becke, *J. Chem. Phys.* **1993**, *98*, 5648; b) A. D. Becke, *Phys. Rev. A* **1988**, *38*, 3098; c) C. T. Lee, W. T. Yang, R. G. Parr, *Phys. Rev. B* **1988**, *37*, 785.

[33] A. Schäfer, C. Huber, R. Ahlrichs, *J. Chem. Phys.* **1994**, *100*, 5829.

[34] a) D. Andrae, U. Haussermann, M. Dolg, H. Stoll, H. Preuss, *Theor. Chim. Acta.* **1990**, *77*, 123; b) F. Weigend, R. Ahlrichs, *Phys. Chem. Chem. Phys.* **2005**, *7*, 3297.

[35] a) D. G. Truhlar, M. S. Gordon, *Science* **1990**, *249*, 491; b) C. Gonzalez, H. B. Schlegel, *J. Phys. Chem.* **1990**, *94*, 5523; c) C. Gonzalez, H. B. Schlegel, *J. Chem. Phys.* **1989**, *90*, 2154; d) K. Fukui, *J. Phys. Chem.* **1970**, *74*, 4161; e) K. Fukui, *Acc. Chem. Res.* **1981**, *14*, 363.

